Physics Letters B 721 (2013) 136–140

Contents lists available at SciVerse ScienceDirect

Physics Letters B

www.elsevier.com/locate/physletb

Neutron matter instabilities induced by strong magnetic fields

R. Aguirre, E. Bauer *

Departamento de Física, Facultad de Ciencias Exactas, Universidad Nacional de La Plata and IFLP-CCT-La Plata, CONICET, Argentina

ARTICLE INFO

Article history:
Received 22 January 2013
Accepted 25 February 2013
Available online 1 March 2013
Editor: W. Haxton

Keywords:
Neutron matter
Magnetic instability

ABSTRACT

We study some properties of spin-polarized neutron matter in the presence of a strong magnetic field at finite temperature. Using the Skyrme model together with the Hartree–Fock approximation we obtain an energy density functional that is employed to extract the spin polarization, the effective mass and the magnetic free energy of the system. In order to find the equilibrium state, we have analyzed different global spin configurations over a wide range of matter density ($0 < n/n_0 \leqslant 3$), magnetic field intensity (10^{14} G $\leqslant B < 10^{19}$ G) and temperature ($T \leqslant 80$ MeV). The outcome is that the system can be either completely spin-down polarized or partially polarized. A change in any of the (n, T, B)-variables can induce a transition from one polarization state to the other. The transition takes place in a surface in the (n, T, B)-phase space, which represents an instability of the system. We have also found a discontinuity in the internal energy associated with this change in the state of magnetization.

1. Introduction

The effects of magnetic fields on dense matter have been a subject of interest from long time ago [1], particularly in relation to astrophysical issues. The equation of state for magnetized matter is important for the neutron star structure [2] and for the cooling of magnetized stars [3–5]. Moreover, since neutrinos are a fundamental piece in cooling processes, its emission and transport properties in the presence of magnetic fields were studied in detail [4,5].

A wide range of observational data of periodic or irregular radiation from localized sources has been related to the presence of very intense magnetic fields in compact stellar objects. These manifestations have been classified as pulsars, soft gamma ray repeaters and anomalous X-ray pulsars, according to the energy released and the periodicity of the episodes. They have been associated with different stages of the neutron star evolution. The intensity of these magnetic fields could reach 10^{14} G in the star surface and could grow up several orders of magnitude in its dense interior. The origin of such unusually large fields is still uncertain. The source of the quasi-periodic frequency observed for the radiation phenomena has been attributed to different causes, such as the breakdown of the star crust or to sudden rearrangements of the magnetization [6]. In any case, a detailed knowledge of the magnetic susceptibility is necessary to clarify this question. As the properties of the radiation measured are closely related to the equation of state of nuclear matter, this subject offers a valuable opportunity to constrain theoretical models.

The study of the high density nuclear equation of state in the presence of very strong magnetic fields and the structure of neutron stars was developed within the covariant field theory (see for example [7,8]). Non-relativistic effective models have also been used in this context, as they are specially suited to deal with dense nuclear systems. In particular, for homogeneous matter they give rise to energy density functionals of low computational complexity. Furthermore, they have been applied to describe non-homogeneous low density environments, such as the neutron star crust.

In this Letter we study infinite homogeneous neutron matter in the presence of an external magnetic field at finite temperature, using the Skyrme model. There are previous works which used the Skyrme model to study neutron matter under similar conditions [9–11]. We consider densities up to three times the normal nuclear density, temperatures up to 80 MeV, and field intensities $10^{14} \leqslant B < 10^{19}$ G, which are appropriate for some astrophysical studies.

The equilibrium state for a system in the presence of an external magnetic field is characterized by a minimum of the appropriate thermodynamical potential [12]. Therefore we examine the possible global configurations of the spin polarization of neutron matter in terms of the field intensity, the density and the temperature.

This Letter is organized as follows. In Section 2 we outline the formalism used to study neutron matter under a strong magnetic field, the outcomes are discussed in Section 3, and the conclusions are drawn in Section 4.

* Corresponding author.
E-mail address: bauer@fisica.unlp.edu.ar (E. Bauer).

0370-2693/$ – see front matter
http://dx.doi.org/10.1016/j.physletb.2013.02.046

2. The Skyrme model for neutron matter in strong magnetic field

The Skyrme model is an effective formulation of the nuclear interaction [13]. It consists of a two-body contact potential plus some terms having an explicit density dependence. Using this interaction and the Hartree–Fock approximation, one builds up an energy density functional. The associated single-particle spectrum can be expressed in such a way that the interaction contributes partly to the definition of an effective mass and partly to a remaining potential energy. This approximation provides a simple and useful scheme to study neutron matter properties like the magnetization, effective mass, etc. There are several parameterizations for the Skyrme model, according to the different applications, which cover issues from exotic nuclei to stellar matter.

We are particularly interested in the contributions coming from terms containing time-reversal-odd densities and currents, since they are active when spin states are not symmetrically occupied. A derivation of these terms can be found in [14].

In working with an external magnetic field B, the energy density functional is the sum of the Skyrme density functional $\mathcal{E}_{Skm}$, plus the interacting term between matter and the magnetic induction B,

$$\mathcal{E} = \mathcal{E}_{Skm} - \mu_N \chi W B, \tag{1}$$

where μ_N is the Bohr magneton, the Lande factor $\chi = -1.913$ takes account of the anomalous magnetic moment and

$$\mathcal{E}_{Skm} = \sum_s \frac{K_s}{2m_s^*} + \frac{1}{16}a\big(n^2 - W^2\big) \tag{2}$$

is the standard Skyrme density functional. Here we have introduced the effective nucleon mass m_s^* for a neutron with spin up $(s = 1)$ or down $(s = -1)$,

$$\frac{1}{m_s^*} = \frac{1}{m} + \frac{1}{4}(b_0 n + s b_1 W) \tag{3}$$

where m is the bare neutron mass, n stands for the neutron number density and W is the spin asymmetry density,

$$W = \sum_s \frac{s}{(2\pi)^3}\int d^3p\, f_s(T,p). \tag{4}$$

The expressions for n and the kinetic density K_s of particles with spin s, are,

$$n = \sum_s \frac{1}{(2\pi)^3}\int d^3p\, f_s(T,p) \tag{5}$$

and

$$K_s = \frac{1}{(2\pi)^3}\int d^3p\, p^2 f_s(T,p). \tag{6}$$

In Eqs. (4)–(6), we have used the statistical distribution function at temperature T,

$$f_s(T,p) = \big[1 + \exp\beta\big(\varepsilon_s(p) - \mu\big)\big]^{-1}, \tag{7}$$

where $\beta \equiv 1/T$, μ is the chemical potential and the particle spectra is,

$$\varepsilon_s(p) = \frac{p^2}{2m_s^*} + \frac{1}{8}v_s - \mu_N \chi s B, \tag{8}$$

which is obtained in a self-consistent way through the functional derivative $\varepsilon_s(p) = \delta\mathcal{E}/\delta f_s(T,p)$. In Eq. (8) we have used,

$$v_s = a(n - sW) + \sum_{s'}\big(b_0 + ss' b_1\big)K_{s'} + \frac{\sigma}{3}t_3(1 - x_3)\big(n^2 - W^2\big)n^{\sigma-1}. \tag{9}$$

The parameters a, b_0 and b_1 can be written in terms of the standard parameters of the Skyrme model,

$$a = 2t_0(1 - x_0) + t_3(1 - x_3)n^\sigma/3,$$
$$b_0 = t_1(1 - x_1) + 3t_2(1 + x_2),$$
$$b_1 = t_2(1 + x_2) - t_1(1 - x_1).$$

Note that W, n and K are all functions of the temperature T, the magnetic field intensity B and the chemical potential μ. The equilibrium state for a system in the presence of a constant magnetic field is given by the stationary configuration of the thermodynamic potential per volume, $U/V = F/V - \mathbf{M}\cdot\mathbf{B}$ [12], where we have introduced the free energy per volume, $F/V = \mathcal{E}_{Skm} - TS/V$ and we have adopted $M = \mu_N \chi W$ for the magnetic moment of the system. Finally the entropy corresponds, in a quasi-particle picture, to

$$S/V = -\sum_s \int \frac{d^3p}{(2\pi)^3}\big[f_s(T,p)\ln\big(f_s(T,p)\big) + \big(1 - f_s(T,p)\big) \times \ln\big(1 - f_s(T,p)\big)\big]. \tag{10}$$

For given values of n, T and B we solve in a self-consistent way the set of Eqs. (3)–(9), obtaining the spin polarization W and the chemical potential μ. Under these conditions the system can be in any of the following global spin configurations: completely polarized state (CPS) or partially polarized state (PPS). In the former case the system is either spin up (CPS-U) with $W/n = 1$ or spin down (CPS-D) with $W/n = -1$, whereas for the latter instance one has $|W/n| < 1$.

As a final remark, note that throughout this article we use units such that $c = 1$, $\hbar = 1$.

3. Results and discussion

In this section we present the results obtained with the Skyrme model, for which the SLy4 parametrization is used. An explicit description of the model parameters can be found, for instance, in Ref. [15]. We extend our analysis to densities up to three times the normal nuclear density, temperatures below $T = 80$ MeV, and the magnetic field intensity within the range $10^{14}\ \mathrm{G} \leqslant B < 10^{19}$ G.

In practice we solve the set of Eqs. (3)–(9) for fixed values of n, T and B, and for each of the three spin configurations CPS-D, CPS-U, and PPS. From these results we select the equilibrium state, which corresponds to the minimum of the thermodynamic potential U. In fact, only a CPS-D or a PPS is obtained. The points where the system changes from one polarization state to other one define a instability surface in the (n, T, B)-space. It is worthwhile to mention that the aim of this contribution is to describe this instability, and we have not considered the possibility of a coexistence of phases. As we have just stated, we have analyzed field intensities from $B = 10^{14}$ G on. However, we do not show results for relatively low field intensities, because a PPS is favored for all the range of densities and temperatures examined. The instabilities start approximately at $B \simeq 3 \times 10^{17}$ G, and become very complex in a neighborhood of $B = 5 \times 10^{18}$ G. Finally, for extreme fields $B \sim 10^{19}$ G they disappear because the system is firmly established in a CPS-D.

To understand the meaning of the instabilities it is convenient to consider the spin asymmetry W in first place. In Fig. 1, we have plotted W as a function of the density for several values of

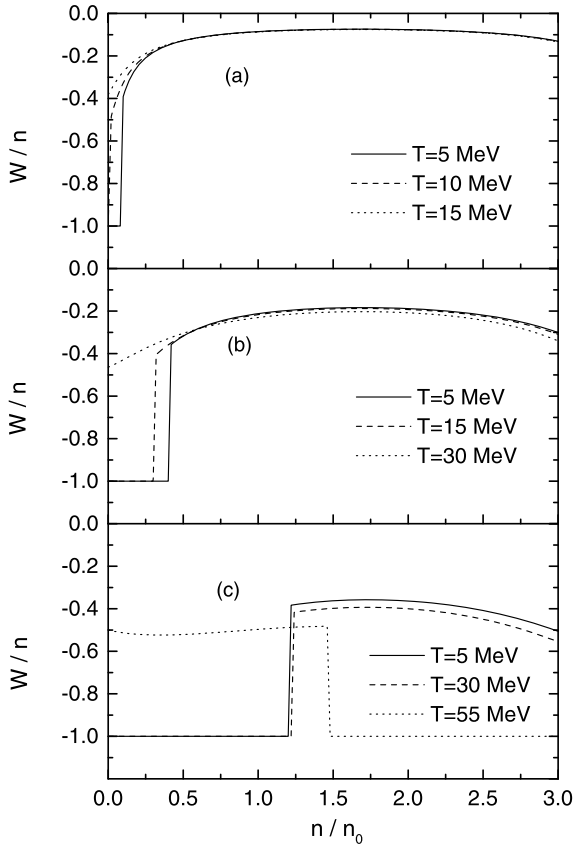

Fig. 1. The ratio of spin asymmetry to particle density W/n as a function of the relative neutron density n/n_0, for several temperatures and the following magnetic intensities $B = 10^{18}$ G (a), $B = 2.5 \times 10^{18}$ G (b), and $B = 5 \times 10^{18}$ G (c). The line convention is explained in each panel. We have adopted $n_0 = 0.16$ fm^{-3}.

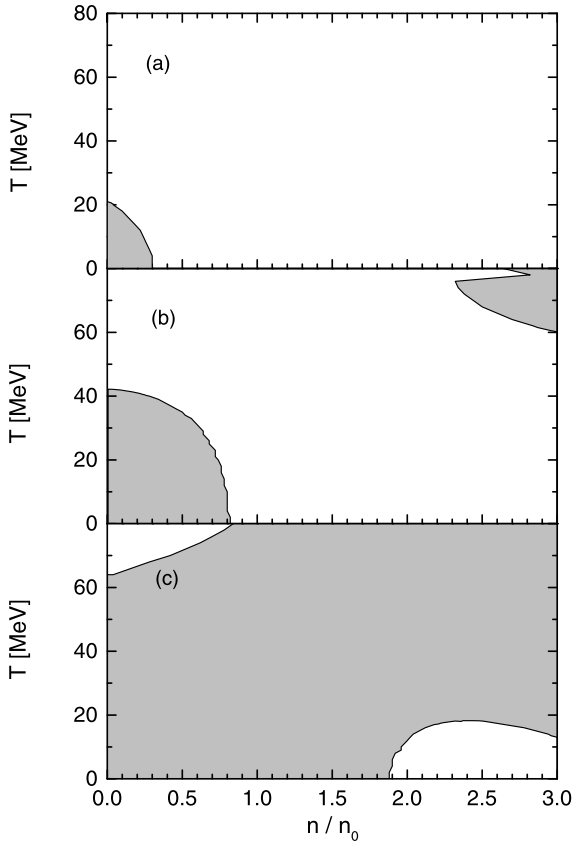

Fig. 2. Instability curves in the (n, T)-plane, for the following magnetic intensities $B = 2 \times 10^{18}$ G (a), $B = 4 \times 10^{18}$ G (b), and $B = 6 \times 10^{18}$ G (c). Shaded (white) areas correspond to CPS-D (PPS) equilibrium regions.

T and B. We have $W/n = -1$ for CPS-D, whereas from the numerical analysis it turns out that $W/n < 0$ for a PPS. From this figure it is evident that the equilibrium state never corresponds to CPS-U ($W/n = 1$), as it is discussed below.

In this figure the cases $B = 10^{18}$ G and 2.5×10^{18} G illustrate the behavior at relatively low external field B. For low temperatures and low densities a CPS-D is the equilibrium configuration, until a threshold density (n_t) where a transition to a PPS is performed. This point is characterized by a sudden change in the slope of the curve. As the temperature grows, the density domain of total polarization is reduced ($n_t \to 0$). Finally, a characteristic temperature T_c is found such that the instability disappears for $T > T_c$ and a PPS is the more stable configuration for all densities.

For the stronger field $B = 5 \times 10^{18}$ G, the situation is modified. A description similar to the previous one still holds for low densities and the temperatures $T = 5$ and 30 MeV. However as the temperature is increased ($T = 55$ MeV) an unexpected CPS-D configuration appears in the high density region.

From these figures we can extract the points which constitute the instability surface. As an illustration, we observe that in Fig. 1(b) there is a break point at $n_t/n_0 = 0.395$ for the slope of the curve corresponding to the temperature $T = 5$ MeV. Therefore $(n_1, T_1, B_1) = (0.395 n_0, 5, 2.5 \times 10^{18})$ is a point of the instability surface. In an analogous way, by scrutinizing Fig. 1(c) one can conclude that $(1.47 n_0, 5, 5 \times 10^{18})$ also belongs to this surface.

It should be noted that the change in the equilibrium configuration always takes place between CPS-D and PPS. It is easy to understand why the CPS-U never is the equilibrium state. It can be demonstrated that for given values of (n, T, B) and particle momentum p, the single particle energy level of an up-state in CPS-U is greater than that of a down-state in CPS-D. Therefore, it requires more energy to accommodate the same number of particles in a CPS-U than in a CPS-D. In addition, the entropy is the same for both configurations, and the matter–field term is positive in the CPS-U and negative in the CPS-D. Hence, the values obtained for $U(n, T, B)$ are always greater in the former case. For this reason in the following we restrict the discussion to PPS and CPS-D.

To complete our description of the phase diagram, we present in Fig. 2 the instability curve in the (n, T)-plane for fixed values of the field B. In order to give a discussion as complete as possible, this figure includes results that extend over the full range of densities and temperatures where applicability of the model is assumed. The range of field intensities is concentrated around $B = 5 \times 10^{18}$ G, where a change of regime is localized. The shaded areas in Fig. 2 correspond to stability of the CPS-D, the outer region corresponds to stable PPS, and the curve in between collects the points of instability. These curves are the traces of the instability surface in the (n, T, B)-space. We observe that for $B = 2 \times 10^{18}$ G there is a single region of CPS-D stability located at the low temperature-low density domain. For the field intensity $B = 4 \times 10^{18}$ G a second region of stability arises for high temperatures and high densities. Finally, for $B = 6 \times 10^{18}$ G these two regions have grown and overlapped. It can be predicted from the last figure that for very large field $B \sim 10^{19}$ G the instability curve will disappear and all the frame will be occupied by a CPS-D.

A deeper understanding can be gained by considering the different components of the magnetic free energy U. We have the kinetic and potential energies in $\mathcal{E}_{Skm}$ (see Eq. (2)), the entropy term $-TS/V$, entering into the free energy F, and the matter–field

interacting term, which is the sum of $(-\mathbf{M}\cdot\mathbf{B})$ plus the last term of Eq. (1). We note that all the contributions are negative, with the exception of the kinetic part. Furthermore all the terms grow in magnitude for increasing density, although with different rates. Beyond these general considerations, we notice that: (i) Within a naif reasoning one expects that the kinetic energy will be minimum for a system having two almost degenerate channels (as for instance spin-up and spin-down) instead of only one. In the present case, however, we found that as the density grows the effective mass becomes increasingly larger in the case of only one spin channel (see the discussion below). As a consequence for sub-saturation densities the minimum of the kinetic term corresponds to a PPS, and changes to a CPS-D for densities around n_0. This behavior is almost independent of T and B. (ii) The potential energy is strictly zero in a CPS-D, while it is negative for a PPS. (iii) As expected, the matter–field interaction term always favors the CPS-D. This trend is emphasized for growing B. (iv) For the entropy term one expects, based on single order–disorder arguments, that it has greater values for the more homogeneous state, which in our study corresponds to the PPS. However, within the Skyrme model and for large enough densities the entropy term favors the CPS-D rather than the PPS. This feature has been already reported in reference [16], where it has been attributed to a distinctive behavior of the Skyrme model. Under those conditions the entropy turns out to be very sensitive to the effective masses corresponding to spin-up or spin-down states. Even though this is an effect mainly driven by the high densities, its influence on the magnetic free energy U is magnified and becomes appreciable for high temperatures.

With these elements at hand, we return to the analysis of the general situation, which has been partially depicted in Figs. 1 and 2. For very low field intensities $B < 3\times 10^{17}$ G, the matter–field term is negligible small ($\mu_N B < 10^{-2}$ MeV) and the behavior of U is dominated by density and thermal effects. Both, kinetic plus potential and entropy terms favors under such circumstances the PPS.

For higher intensities 3×10^{17} G $< B < 3\times 10^{18}$ G, as illustrated by Fig. 1(a), (b) and Fig. 2(a), the matter–field interaction turns out to be relevant. Hence for low density and temperature, it prevails over the potential energy (mainly density-dependent) and the entropy effect (mainly thermal dependent) leading to a CPS-D. Thus the predominance of this CPS is restricted by two effects. As the temperature increases, the entropy term becomes important and changes the global polarization into a PPS. On the other hand, as the density grows the potential energy takes control, inducing a change towards a PPS. Note that for medium and high densities the kinetic term favors a CPS-D configuration, but the potential energy of a PPS is negative and stronger. Let us recall that the potential energy contribution is zero for a CPS. As B grows within this interval, the magnetic term is strengthened and consequently the CPS-D region is extended up to higher densities and temperatures, see Fig. 1(b).

There is a small neighborhood of $B = 5\times 10^{18}$ G where a new effect becomes visible, as shown in Fig. 1(c) and Fig. 2(b). At the temperatures $T = 5$ and 30 MeV, of Fig. 1(c), there is no significative modifications. However for high enough temperatures the anomalous behavior of the entropy becomes relevant. The effect is evident for the $T = 55$ MeV case in Fig. 1(c) and for $T \geqslant 60$ MeV in Fig. 2(b). For high densities the entropy plus magnetic terms prevails over the kinetic plus potential terms, leading to a CPS-D.

A further increase in B, as illustrated in Fig. 2(c), reinforces the influence of the matter–field interaction. The system is not completely polarized yet, as two PPS-stability regions still remains. One of them is located at low densities and high temperatures and the other one at high densities and low temperatures. The first one is supported by the high temperature entropy contribution. In the latter case the entropy has no significant influence and the potential term overcomes the kinetic and magnetic contributions. However, as the temperature is increased, the anomalous behavior of the entropy becomes important and thus the CPS-D is restored.

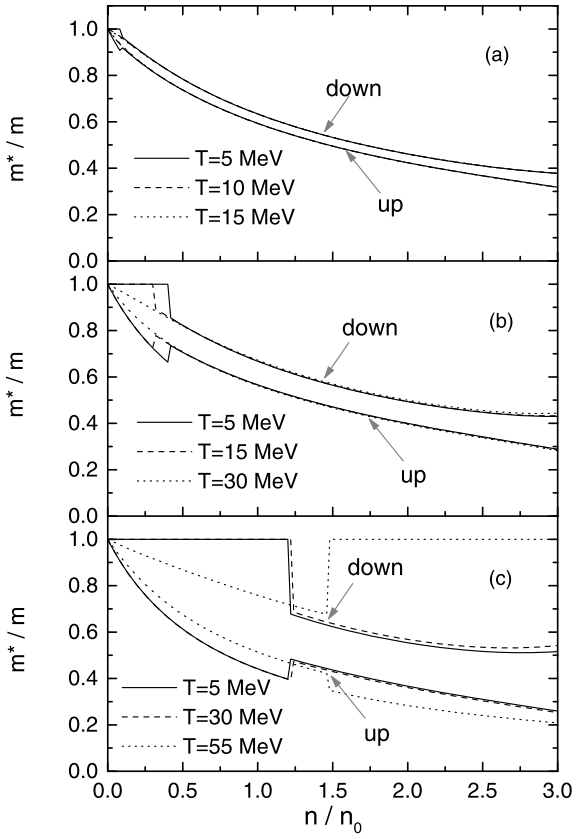

Fig. 3. The effective to bare neutron mass quotient as a function of the relative density for several temperatures and the following magnetic intensities $B = 10^{18}$ G (a), $B = 2.5\times 10^{18}$ G (b), and $B = 5\times 10^{18}$ G (c). The line convention is explained in each panel. In each panel the upper (lower) family of curves correspond to spin-down (spin-up) states.

We turn now to the analysis of the effective nucleon mass, which has an important role in the selection of the physical configuration. It has also others interesting applications, as for example in the study of transport properties. We devote Fig. 3 to present its density dependence for several temperatures and field intensities. From these figures we can see that the spin-up effective mass has always smaller values than the spin-down one. Furthermore in the PPS, both are decreasing functions of the density, whereas $m_d^* = m$ in the CPS-D. This is an effect due to the numerical values of the model parameters. As a consequence, for intermediate and high densities there is a pronounced difference in the effective mass of states in a CPS or a PPS. In turn this is the cause that the kinetic integral has a lighter weight in a CPS than in a PPS. Consequently the kinetic contribution of a CPS is significantly reduced as compared with that of a PPS.

The discontinuities in this figure indicate the instability points. They clearly signalize the change of the thermal regime in the $B = 5\times 10^{18}$ G case (Fig. 3(c)). For temperatures $T = 5$ and 30 MeV, the value $m_d^* = m$ is attained at low densities, whereas for high temperatures ($T = 55$ MeV) it corresponds to the high density region.

As a final application, we consider here the energy difference for neutron matter crossing the instability surface. One must bear in mind that U remains unchanged across such surface, but the internal energy (given by Eq. (1)), could has a discontinuity. This

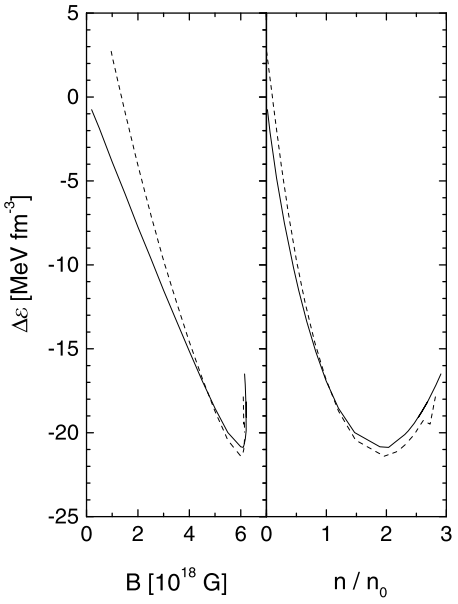

Fig. 4. The energy density difference across the instability surface as a function of the field intensity (left panel) and the relative density (right panel). We have considered the low temperatures $T = 0.1$ MeV (solid lines) and $T = 10$ MeV (dashed lines).

quantity is of interest in astrophysical studies, since the energy released in magnetic phase transitions has been addressed as a possible cause of the sudden episodes in magnetars [6].

We show in Fig. 4 the difference $\Delta\mathcal{E}$ in the energy density between a PPS and a CPS-D in a instability point, for temperatures $T = 0.1$ and 10 MeV, as a function of the field intensity (left panel) or the particle density (right panel). For the temperatures considered, the PPS is stable for densities above the instability point. The magnitude of the difference increases with B, and for extreme values the curves become bivaluated. This is a consequence of the fact that for low temperatures and high B we found two instability points located at low and high density (see Fig. 2(b)). As a function of n, a minimum value is obtained for $n/n_0 \simeq 2$. It can be appreciated that for $T = 0.1$ MeV, a decrease of energy is found when the system goes from CPS-D to PPS. Instead, for $T = 10$ MeV there exist a region of moderate B and very low n for which an energy increase takes place.

Before we end this section, we want to mention some approximations in the present study that deserve a more detailed study. In first place some features shown here are strongly model-dependent, such as the effective mass and the anomalous behavior of the entropy at high densities. It will be desirably a contrast with other theoretical formulations, as for example relativistic hadronic models [17]. In second place we have disregarded possible effects due to the anisotropic pressure (see [11,18], and references therein). This is an issue intensively studied nowadays, which could have considerable consequences for very intense fields. Finally, the inclusion of other hadrons and leptons is appropriate for the study of neutron star matter. All these points and its relations with the magnetic instabilities will be developed in further investigations.

4. Conclusions

In the present contribution we have discussed the existence of magnetic instabilities in homogeneous neutron matter at finite temperature under the presence of an external magnetic field. For this purpose we have used the SLy4 parametrization of the Skyrme model within the Hartree–Fock approximation. We have studied the equilibrium configuration for a wide range of densities, temperatures and field intensities. We have paid special attention to some key properties such as the effective neutron mass and the global spin asymmetry. We have found that within our approach, magnetic instabilities develop for field intensities $B > 3 \times 10^{17}$ G and disappear near $B \sim 10^{19}$ G. Different density and thermal effects produce a change between completely and partially spin-polarized matter. Thus a complex description of the instability surface in the (n, T, B)-space is obtained. Some unexpected results arise as a consequence of the high density behavior of the entropy. Although for more of the cases an increase of the temperature favors a partially polarized configuration, this is not the case for very strong fields. Led by the anomalous entropy behavior, neutron matter prefers a completely polarized state at high temperatures, even though the magnetic field is not strong enough.

Finally, we have considered the energy release across the magnetic instability. For this purpose we have evaluated the difference in the internal energy between the final and initial equilibrium states. We have found that for low temperatures it is an increasing function of the magnetic field intensity, while as a function of the density it exhibits a maximum value near $n/n_0 = 2$.

We expect that these results will be of interest for the study of compact stellar objects under the influence of strong magnetic fields. However, the application to astrophysical objects requires some further refinements, such as the incorporation of others kinds of particles (protons, hiperons and electrons), higher order B-terms and a test with others interactions. Related investigations are in progress.

Acknowledgements

This work has been partially supported by the CONICET, under contract PIP 0032 and by the Agencia Nacional de Promociones Cientificas y Tecnicas under contract PICT-2010-2688.

References

[1] D. Lai, Rev. Mod. Phys. 73 (2001) 629.
[2] J.M. Lattimer, M. Prakash, Phys. Rep. 442 (2007) 109.
[3] Y.A. Shibanov, D.G. Yakovlev, Astron. Astrophys. 309 (1996) 171.
[4] D.G. Yakovlev, A.D. Kaminker, O.Y. Gnedin, P. Haensel, Phys. Rep. 442 (2001) 1, and references therein.
[5] V.G. Bezchastnov, P. Haensel, Phys. Rev. D 54 (1996) 3706;
D.A. Baiko, D.G. Yakovlev, Astron. Astrophys. 342 (1999) 192;
D. Chandra, A. Goyal, K. Goswami, Phys. Rev. D 65 (2002) 053003.
[6] I.S. Suh, G.J. Mathews, arXiv:1005.2139, 2010.
[7] S. Chakrabarty, D. Bandhyopadhyay, S. Pal, Phys. Rev. Lett. 78 (1997) 2898.
[8] A. Broderick, M. Prakash, J.M. Lattimer, Astroph. J. 537 (2000) 351.
[9] M.A. Perez Garcia, Phys. Rev. C 77 (2008) 065806.
[10] A.A. Isaev, J. Yang, Phys. Rev. C 80 (2009) 065801.
[11] A.A. Isayev, J. Yang, Phys. Lett. B 707 (2012) 163.
[12] H.B. Callen, Thermodynamics an Introduction to the Physical Theories of Equilibrium Thermostatistics and Irreversible Thermodynamics, John Wiley and Sons, New York, 1960.
[13] M. Bender, P.H. Heenen, Rev. Mod. Phys. 75 (2003) 121.
[14] M. Bender, J. Dobaczewski, J. Engel, W. Nazarewicz, Phys. Rev. C 65 (2002) 054322.
[15] F. Douchin, P. Haensen, J. Meyer, Nucl. Phys. A 665 (2000) 419.
[16] A. Rios, A. Polls, I. Vidaña, Phys. Rev. C 71 (2005) 055802.
[17] J. Dong, U. Lombardo, W. Zuo, H. Zhang, Nucl. Phys. A 898 (2013) 32.
[18] A. Perez Martinez, H. Perez Rojas, H. Mosquera Cuesta, Int. J. Mod. Phys. D 17 (2008) 2107;
E.J. Ferrer, V. de la Incera, J.P. Keith, I. Portillo, P.L. Springsteen, Phys. Rev. C 82 (2010) 065802.